Talanta 81 (2010) 228–234

Contents lists available at ScienceDirect

Talanta

journal homepage: www.elsevier.com/locate/talanta

A Clark-type oxygen chip for *in situ* estimation of the respiratory activity of adhering cells

Ching-Chou Wu[a,b,*], Hsiang-Ning Luk[c], Yen-Ting Tsai Lin[a], Chia-Yin Yuan[a]

[a] *Department of Bio-industrial Mechatronics Engineering, National Chung Hsing University, No. 250, Kuo Kuang Road, Taichung 402, Taiwan*
[b] *Institute of Biomedical Engineering, National Chung Hsing University, No. 250, Kuo Kuang Road, Taichung 402, Taiwan*
[c] *Anesthesiology Department, Taichung Veterans General Hospital, No. 160, Sec. 3, Chung Kang Road, Taichung, Taiwan*

ARTICLE INFO

Article history:
Received 12 September 2009
Received in revised form
24 November 2009
Accepted 29 November 2009
Available online 3 December 2009

Keywords:
Clark-type
Oxygen chip
Sol electrolyte
Oxygen consumption
Respiration activity

ABSTRACT

A Clark-type oxygen chip consisting of a polydimethylsiloxane (PDMS) reservoir containing an amino group-modified PDMS oxygen-permeable membrane (OPM) and a glass substrate containing a three-electrode detector has been constructed by using microfabrication techniques, and it is utilized for *in situ* measurement of the respiration activity of adhering cells. Use of the alginate sol electrolyte and the electroplating Ag/AgCl pseudo-reference electrode can effectively diminish the crosstalk between the electrochemical electrodes and supply a stable potential for the detection of dissolved oxygen, respectively. The Clark-type oxygen chips possess only 1.00% residual current, response time of 13.4 s and good linearity with a correlation coefficient of 0.9933. The modification of amino groups for the OPM obviously facilitates the adhesion of HeLa cells onto the PDMS OPM surface and allows the cells to spread after 2 h of incubation. The oxygen consumption of the cells in the cell-adhesion process increases with the adhesion time, and the increment of cellular oxygen consumption per minute reaches a maximum after 30 min of incubation. Moreover, the change in the respiration activity of adhering HeLa cells stimulated by the high concentration of glucose or propofol anaesthetic can be monitored in real time with the Clark-type oxygen chip.

1. Introduction

Cells are the essential functional and integrative units of living organisms. Cells intake nutrients and oxygen to produce cellular energy (adenosine triphosphate, ATP) as part of what is termed the catabolic pathway, and they excrete heat and acidic waste products to maintain life. Therefore, the measurement of cellular metabolism-related molecules is important for the estimation of cell activity, and it allows us to analyse the physiological responses that cells have to extrinsic chemical or physical stimulations. The measurement of cell activity is profoundly meaningful for clinical diagnostics, pharmacological drug screening, tumour chemosensitivity tests and environmental toxicant monitoring.

Recently, there have been many efforts to develop non-invasive methods for monitoring cell activity with planar microsensors because of the sensitive area of miniaturised electrodes that is easily accessible to the cell surface [1–3]. For example, a microphysiometer system (Cytosensor® Microphysiometer, Molecular Devices, Inc.) is commercially available for the measurement of the extracellular acidification rate based on light-addressable potentiometric sensors [4]. Ion-sensitive field effect transistors (ISFETs) [5–7] and iridium oxide microelectrodes [8,9] are the other famous pH-sensitive detectors for the assessment of the extracellular acidification of living cells. Wolf and co-workers have also developed the multiparametric microsensor chip, which can simultaneously record the cellular respiration rate with amperometric oxygen electrodes, the extracellular acidification rate with ISFETs and the cell-adhesion behaviour with impedimetric interdigitated electrodes [7,10–12]. Moreover, multiparametric microsensors were used for the practical evaluation of the chemosensitivity of living tumour cells [13–15]. Among the metabolism-related processes assessed, the change in the amount of dissolved oxygen consumed by the cells is an important index for the cellular respiration activity because the oxygen consumption of cells corresponds directly to the activity of the mitochondrial respiratory chain [16].

The Clark-type oxygen electrode is a well known design capable of specifically measuring the dissolved oxygen concentration of media without an external interference. In Wolf's early studies, a Clark oxygen electrode was externally inserted into the fluid exit port of a cell chip to *ex situ* measure the respiration activity of cells [10,13,14]. Heimburg et al. developed a Clark oxygen electrode integrated into a thermostat chamber to compare the difference in

* Corresponding author at: Department of Bio-industrial Mechatronics Engineering, National Chung Hsing University, No. 250, Kuo Kuang Road, Taichung 402, Taiwan. Tel.: +886 4 2285 1268; fax: +886 4 2287 9351.
E-mail address: ccwu@dragon.nchu.edu.tw (C.-C. Wu).

0039-9140/$ – see front matter © 2009 Elsevier B.V. All rights reserved.
doi:10.1016/j.talanta.2009.11.062

oxygen consumption between undifferentiated and differentiated preadipocyte suspensions [17]. However, to the best of our knowledge, no planar Clark-type oxygen sensor has been integrated with the cell chip for *in situ* measurement of the oxygen consumption of adhering cells [11,12,15,18]. Although Bionas GmbH Inc. claims that their Bionas® metabolic chip equips the modified Clark-type sensors [15,19], the amperometric oxygen sensors of the metabolic chip are not really compatible with the Clark-type configuration due to their lack of an oxygen-permeable membrane (OPM) used to separate the electrodes and electrolyte from the complicated culture medium. In a non-Clark-type design, the reduction current of dissolved oxygen is easily interrupted by contamination of the electrode surface by cell adhesion or protein adsorption and the change in electrolyte composition caused by the cellular metabolic products or electroactive chemicals. The signal perturbation results in the lower specificity and lower stability of sensors [11].

The first planar Clark-type oxygen chip made by standard microfabrication techniques was developed by Koudelka [20]. Suzuki and co-workers successively improved the silicon-based fabrication processes and the sensing characteristics of chips by incorporating several new features into the design. These included the separate three-electrode configuration connected by a narrow groove in order to reduce the electrochemical crosstalk, the slit-designed Ag/AgCl reference electrode capable of increasing the lifetime and supplying a more stable potential, the use of gel electrolytes and new techniques for bonding the OPM to the detector substrate [21–28]. Furthermore, Wu et al. constructed a novel glass-based Clark-type oxygen chip by bonding the glass substrate containing amperometric electrodes to the polydimethylsiloxane (PDMS) reservoir immobilised with an OPM [29]. However, the aforementioned Clark-type oxygen chips [20–29] could not perform the *in situ* measurement of the respiratory activity of adhering cells due to the hydrophobic property of OPM that is adverse to cell adhesion.

Essentially, a planar Clark-type oxygen chip capable of measuring the respiration activity of adhering cells needs to satisfy the requirements including a transparent substrate for optical observation, good sensing characteristics for detection of dissolved oxygen and appropriate biocompatibility of OPM surface for cell growth. Therefore, an improved glass-based Clark-type oxygen chip is fabricated in the study, and an alginate sol electrolyte and a Ag/AgCl-electroplated pseudo-reference electrode are used to promote the sensing characteristics of the chip. Moreover, the PDMS-made OPM surface is modified with amino groups to facilitate cell adhesion and growth [30,31]. The effects of the OPM modification, the sol electrolyte and the Ag/AgCl pseudo-reference electrode on the detecting properties of Clark-type oxygen chips are discussed in detail. Moreover, the respiration activity of human cervical cancer cells (HeLa) adhering to the surface-modified OPM is estimated *in situ* with the Clark-type oxygen chip.

2. Experimental

2.1. Chemicals

Tris(hydroxymethyl) aminomethane (Tris) was obtained from United States Biological (MA). Potassium chloride (KCl), silver nitrate ($AgNO_3$) and sodium sulphite (Na_2SO_3) were purchased from Showa (Japan). 3-Aminopropyltrimethoxysilane (APTS), potassium nitrate (KNO_3), nitric acid (HNO_3), sodium alginate (low viscosity) and iron(III) chloride hexahydrate ($FeCl_3{\cdot}6H_2O$) were purchased from Sigma. Sulphuric acid (H_2SO_4, Wako, Japan) and hydrogen peroxide (H_2O_2, Wako, Japan) were used for cleaning the slide glasses, and 2-propanol (Kanto Chemical, Japan) was used for cleaning the polyacrylate materials. All solutions were prepared with double distilled water purified through a Milli-Q system. All chemicals were of reagent grade and were used without further purification.

2.2. Chip fabrication

The oxygen chip is composed of a PDMS reservoir with an immobilised PDMS OPM and a glass substrate with a three-electrode detector as shown in Fig. 1A. The glasses were first cleaned by immersing them in Piranha solution (7:3, v/v) of 96% H_2SO_4 and 30% H_2O_2) at 80 °C for 30 min. The lift-off technique was used to pattern the electrode geometry on the glass substrate. 50 nm Ti and 250 nm Au were sequentially sputter-deposited to construct the working, reference and counter electrodes. Subsequently, a 24-μm thick insulator layer, fabricated using a SU8-3025 negative photoresist (MicroChem, MA) with 2000 rpm for 30 s, was used to define the sensitive area of the electrodes and simultaneously form a groove for the filling of the electrolyte. The width of groove around the working electrode, counter electrode and reference electrode was 100 μm, 200 μm and 200 μm, respectively. The area of the working electrode was 20 μm × 20 μm and that of the counter and reference electrodes was 200 μm × 2 mm.

The OPM was prepared from a PDMS (Sylgard 184, Dow Corning, MI)-curing agent mixture (10:1, w/w) because of its good oxygen permeability [29]. Moreover, toluene was added to the PDMS mixture to adjust its viscosity in order to obtain PDMS membranes of the desired thickness. Flat polyacrylate plates were cleaned using 2-propanol with sonication for 5 min. The PDMS–toluene mixture (2:1, v/v) was spread on the clean polyacrylate plate, spun at 3000 rpm for 60 s and then cured on a hot plate at 60 °C for 30 min

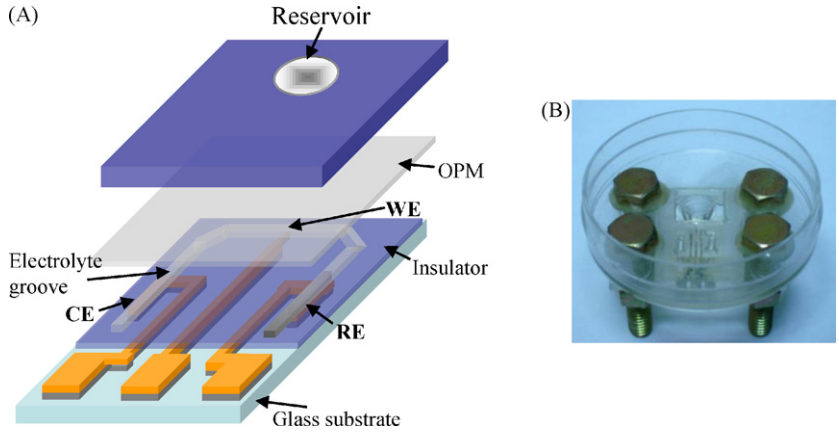

Fig. 1. (A) Schematic diagram of a Clark-type oxygen chip construction. (B) A bonded Clark-type oxygen chip fixed by a home-made clamp. WE: working electrode, RE: reference electrode, CE: counter electrode, and OPM: oxygen-permeable membrane.

to form a 15-μm thick membrane. The PDMS reservoir was made of a PDMS slab by drilling a 3-mm diameter hole, which regulated the sensitive area of the oxygen sensor. The PDMS-reservoir substrate was cut into dimensions suitable to fit the size of the detector glass substrate. Subsequently, both the PDMS membrane and the PDMS reservoir were simultaneously treated with O_2 plasma (Femto, Diener Electronic, Germany) with 100 W for 15 s. The PDMS reservoir was then placed on the O_2 plasma-treated membrane formed on the polyacrylate plate. Irreversible cross-linking between the O_2 plasma-treated surfaces produced a strong adhesion of the two PDMS materials. Finally, the reservoir slab was peeled off of the PDMS-coated plate. The irreversible adhesion between the PDMS materials gave the reservoir an OPM at the bottom. In order to improve the cell adhesion on the PDMS OPM, the hydrophobic surface of the OPM needed to be modified with amino groups [30]. First, the OPM-bonded reservoir was treated with O_2 plasma (100 W, 10 s) so as to display hydroxyl groups on the surface of the OPM. 20 μl of APTS solution (1%, v/v) dissolved in acetone was dropped into the reservoir for 3 h. After silanisation, the reservoir was sequentially rinsed with acetone and double distilled water to remove the unbound residues of APTS. Afterward, the modified reservoir was kept in a humidity-controlled case (15% relative humidity) at room temperature for 1 day to gently evaporate the acetone molecules absorbed onto the PDMS substrate.

2.3. Fabrication of the Ag/AgCl pseudo-reference electrode

In the three-electrode detector, a thin-film Au electrode with a Ag/AgCl-deposited layer was used as a pseudo-reference electrode. The electroplating of the silver layer was accomplished in a 100 mM HNO_3/KNO_3 mixture (pH 1.0) containing 10 mM $AgNO_3$ at −0.28 V for 10 min by using a three-electrode cell at room temperature. Two platinum wires were used separately as the quasi-reference and counter electrodes. Following the silver electroplating, the Ag-electroplated Au electrode was instantly immersed in the 100 mM $FeCl_3$ solution for 10 min to chemically form the AgCl layer [32]. The potential stability of the Ag/AgCl pseudo-reference electrodes was estimated in 25 mM Tris buffer (pH 10.5) containing 100 mM KCl using the open-circuit potential (OCP) method with a potentiostat (CHI842B, CH Instruments, TX) versus a commercially available Ag/AgCl macro-reference electrode (3 M KCl, CHI111, CH Instruments, TX).

2.4. Electrolyte filling and chip bonding

After drilling the inlets of the internal electrolyte in the PDMS-reservoir slab, the slab and the detector glass substrate were aligned under a microscope. The flat PDMS slab and the insulator-coated glass substrate could naturally form the reversible sealing. Then, a 25 mM Tris buffer (pH 10.5) containing 100 mM KCl and 2% sodium alginate (w/w), used as the internal electrolyte, was filled into the long narrow groove. First, a water layer covered the OPM surface, which could prevent masses of gas from penetrating into the electrolyte groove during the application of suction. Subsequently, one of the inlets was filled with the electrolyte, and the other inlet was subjected to suction with a pump so as to affect the electrolyte filling. In addition, a home-made clamp comprising a petri dish and a polyacrylate plate was used to facilitate the mechanical fixation between the PDMS-reservoir slab and the glass substrate during the experimental operation, as shown in Fig. 1B. A 4 mm × 4 mm window was cut into the bottom of the petri dish with a CO_2 laser engraving machine (Venus V-12, Laser-Pro, GCC, Taiwan), which was aligned with the reservoir inlet. The design allows for an increase in media volume for a long-term cell culture.

2.5. Sensor characteristics

A three-electrode system connected with a potentiostat (CHI842B, CH Instruments, TX) was adopted to estimate the characteristics of the oxygen sensor. Amperometry was used to quantify the dissolved oxygen concentration by calculating the oxygen reduction current. Solutions with varied dissolved oxygen concentrations were added in the oxygen-sensing area of the reservoir to test the linearity at room temperature. The different oxygen concentrations of the solutions were adjusted by adding Na_2SO_3 or bubbling oxygen [24,29] and simultaneously calibrated with a commercially available oxygen meter (Oxi330i, WTW, NY). Furthermore, a 100 mM Na_2SO_3 solution at zero-oxygen concentration was repetitively added to the reservoir with the oxygen chip to test the reproducibility in air.

2.6. Cell preparation and measurement of respiration activity

The human cervical cancer cell line (HeLa, ATCC No. CCL2) was a gift from Dr. Ming-Jer Tang (National Cheng Kung University, Taiwan) and was regularly maintained in Dulbecco's modified Eagle's medium (DMEM, SAFC-Biosciences, KS) containing 4.5 g/l glucose, 5% foetal bovine serum (HyClone, UT) and 1% penicillin–streptomycin (HyClone, UT) in a 37 °C humidified incubator with 5% CO_2. Before measuring the respiration activity of the HeLa cells, they were harvested and suspended in DMEM solution. At the same time, the number of viable cells was determined using the trypan blue assay.

In general, most mammalian cells need to adhere to and spread on a substrate to maintain normal growth. The respiration activity of cells in the cell-adhesion process was evaluated by measuring the depletion of dissolved oxygen (oxygen consumed by the cells). The Clark-type oxygen chips were sterilised with 70% ethanol, cleaned with pure water and placed in a humidity-saturated incubator (37 °C, 5% CO_2) during the experiments. A 10 μl cell suspension with a density of 3×10^5 cells/ml was placed, following the addition of 50 μl DMEM solution, in the reservoir with the Clark-type oxygen chip. Then, the dissolved oxygen concentration of the media was time-lapse recorded to verify the oxygen consumption of cells in the cell-adhesion process. When measuring the effect of chemicals on the respiration activity of the cells, the HeLa cells (with a density of 4.3×10^2 cells/mm^2) were seeded on the surface of APTS-modified OPM and cultured for 18 h. Before performing the drug test, only 15 μl DMEM solution was left in the reservoir. Subsequently, 10 μl of stimulants, such as 100 mM glucose prepared in Dulbecco's phosphate-buffered saline (HyClone, UT) and propofol (Bayer Schering Pharma, Germany), an intravenous anaesthetic, were added and the respiration activity of the cells was estimated *in situ*.

3. Results and discussions

3.1. Properties of Ag/AgCl pseudo-reference electrode

The Ag/AgCl electrode is a well developed reference electrode, with advantages that include a low dependence on the temperature, independence from the pH value of the electrolyte and good compatibility with microfabrication techniques [20,24,25,28,32]. The planar silver films could be formed by sputtering [20,24,28] or electroplating [32]. Polk et al. found that the potential stability and lifetime of the Ag/AgCl electrode is positively proportional to the thickness and surface area of the Ag/AgCl film [32]. In general, the thickness of the physically sputtered or evaporated silver layer is only on the scale of several hundred nanometres. In contrast to thin-film microfabrication, the electroplating technique

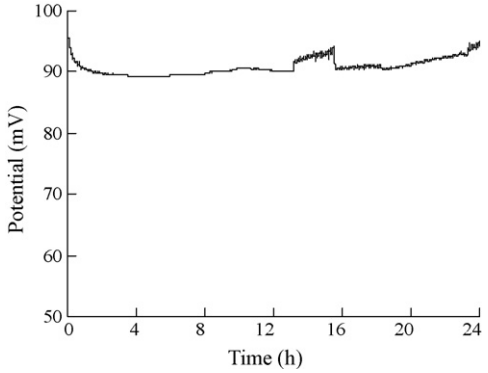

Fig. 2. Open-circuit potential of the electroplated Ag/AgCl pseudo-reference electrode measured for 24 h in 25 mM Tris buffer (pH 10.5) with 100 mM KCl vs. a commercially available Ag/AgCl reference electrode.

allows us to easily and inexpensively obtain a thicker silver layer on the micrometer scale. Therefore, we electroplated a silver layer at −0.28 V for 10 min in the 100 mM HNO_3/KNO_3 mixture (pH 1.0) containing 10 mM $AgNO_3$. The thickness of the electroplated silver layer, measured by a stylus profilometer, was 3.11 ± 0.02 μm. The electroplated Ag layer was instantly dipped into a 100 mM $FeCl_3$ solution for 10 min to form the AgCl layer chemically [32]. The stability of the Ag/AgCl electrode was estimated by using OCP in 25 mM Tris buffer containing 100 mM KCl (whose composition is similar to the internal electrolyte of the Clark-type oxygen chip) versus a commercially available Ag/AgCl reference electrode, as shown in Fig. 2. The potential variation within 24 h was 5.9 ± 3.9 mV, statistically calculated with three repetitions, and the drift rate was approximately close to that of Polk et al.'s study (a potential variation of 4 mV within 17 h) [32]. Furthermore, the potential can be stably maintained for at least 40 h. The potential stability and lifetime of the electroplated thick-film Ag/AgCl electrode is better than that of the thin-film Ag/AgCl electrodes that were fabricated without the protection of a complicated slit structure [23,24] and a miniaturised liquid junction [25]. In summary, the good potential stability and lifetime of the electroplated Ag/AgCl electrode is attributed to the relatively large amount of available Ag/AgCl with the 3.11 μm thickness and the 4×10^5 μm^2 geometric area. The potential properties of the electroplated Ag/AgCl electrode could be used as a good pseudo-reference electrode for the detection of cellular respiration activity.

3.2. Sensor characteristics

3.2.1. Cyclic voltammogram

The electrochemical behaviour of oxygen reduction measured in the Clark-type oxygen chip was investigated. Fig. 3 shows the typical cyclic voltammogram of oxygen reduction performed in an air-filled reservoir from 0 V to −1.0 V with a 20 mV/s scanning rate. The diffusion-limited current for oxygen reduction appeared in the potential range of −0.6 V to −0.8 V, indicating that the reduction current measured in the potential range can be quantified to proportionally obtain the oxygen concentration. When negatively increasing the potential, the hydrogen evolution took place after −0.85 V. Therefore, we employed a −0.7 V potential to evaluate the sensing characteristics of the Clark-type oxygen chip.

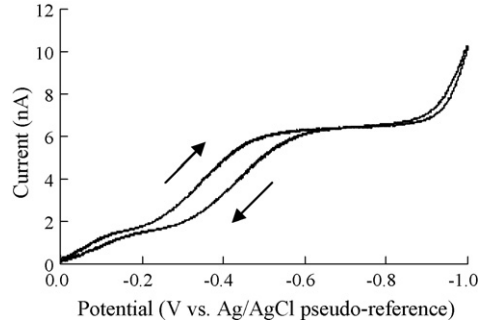

Fig. 3. Cyclic voltammogram of oxygen reduction was measured in an air-filled reservoir from 0 V to −1.0 V with a scanning rate of 20 mV/s.

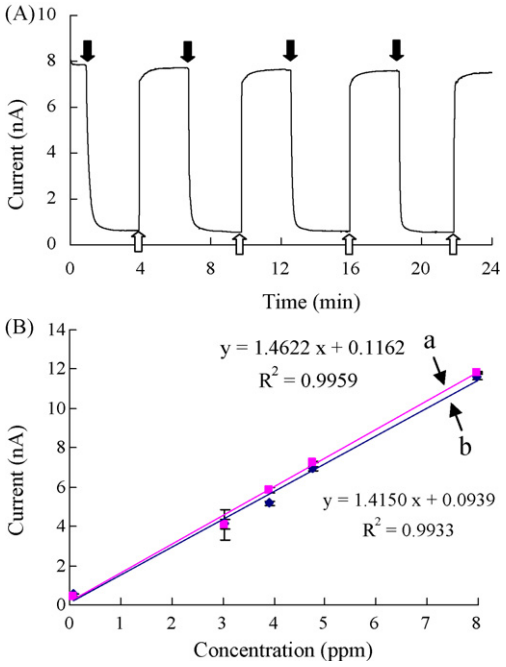

Fig. 4. (A) The response curve of the Clark-type oxygen chip was fulfilled with the periodic, consecutive injection and suction of the zero-oxygen solution in the membrane-separated reservoir at −0.7 V vs. a thick-film Ag/AgCl pseudo-reference electrode with a 15 μm oxygen-permeable membrane. Solid and blank arrows show the reservoir with and without the addition of zero-oxygen solution, respectively. (B) The calibration curves for the Clark-type oxygen chip without (curve (a)) and with (curve (b)) APTS modification for the oxygen-permeable membrane.

3.2.2. Response curve

A 100 mM Na_2SO_3 solution with a zero-oxygen concentration was employed to repetitively test the reproducibility and response time [23]. Fig. 4A shows the reduction in oxygen relative to the periodic injection and suction of the zero-oxygen Na_2SO_3 solution in the membrane-separated reservoir of the Clark-type oxygen chip. When the Na_2SO_3 solution was filled in the reservoir, only a small reduction current was observed, indicating that the Na_2SO_3 solution effectively removes most of the oxygen around the sensitive area of the working electrode. On the other hand, an obvious reduction current was observed in the air-filled reservoir due to the fast diffusion of oxygen from the air to the electrolyte. The current difference with and without the Na_2SO_3 solution in the reservoir was 7.09 ± 0.09 nA, with a relative standard deviation (RSD) of 1.21%. The small RSD implies that the oxygen chip is capable of good reproducibility. Moreover, the use of the APTS-modified OPM and sol electrolyte do not affect the reproducibility, as evidenced by the fact that the RSD is almost the same as that of Wu et al.'s study with the similar chip design [29]. Additionally, the baseline drift of reduction current in the air-filled state within 24 min was only 0.26 nA, being about 3.33% drift-normalised by the 7.82 nA baseline current. The good reproducibility and small baseline drift are attributed to the stable potential of thick-film Ag/AgCl reference electrodes and the alginate sol electrolyte with less electrode crosstalk.

The 90% response time of the Clark-type oxygen chip was 13.4 s, which is longer than that (8.7 s) of Wu et al.'s result with the same 15-μm thick OPM [29]. This phenomenon is attributed to the effects of the APTS modification of the OPM and the viscosity of the alginate sol electrolyte on the response time. Shiku et al. proved that the modification of polar functional groups for the hydrophobic PDMS surface decreases the mass-transfer rate constant of oxygen from the water phase to the PDMS phase [33]. Therefore, the APTS modification (NH_2 group) of the OPM surface retards the transport rate of oxygen at the OPM-solution interface. Furthermore, the 2% (w/w) sodium alginate dissolved in the electrolyte obviously increases the solution viscosity, which has the reciprocal relation to the diffusion coefficient of oxygen according to the Wilke–Chang equation [34]. Therefore, the high viscosity of alginate sol electrolyte gives rise to a smaller diffusion coefficient for oxygen, resulting in an increase in response time [35].

3.2.3. Calibration curve

The solutions of different dissolved oxygen concentration were placed in the reservoir with the Clark-type oxygen chip to measure the calibration curve. Fig. 4B shows the calibration curves of the Clark-type oxygen sensors with or without the APTS modification for the OPM. Both curves presented good linearity, with correlation coefficients of 0.9933 and 0.9959, with and without the APTS modification, respectively. This was due to the low electrochemical crosstalk between electrodes. The slope of the calibration curve obtained from the APTS-unmodified oxygen sensor is slightly larger than that obtained from the APTS-modified oxygen sensor. This implies that the APTS modification of the OPM insignificantly affects the oxygen permeability of the PDMS membrane. The average residual currents for zero-oxygen concentration calculated from the APTS-unmodified and APTS-modified oxygen sensors, respectively, were 0.79% and 1.00% of the current measured in the solution containing 7.9 ppm oxygen concentration. The residual current of the oxygen chips is much smaller than that (18%) of Wu et al.'s results [29] and similar to that of Suzuki's study using the alginate gel electrolyte and the groove-connected electrode configuration [23,24]. The small residual current measured in the Clark-type oxygen chip is attributed to the smaller oxygen influx from the groove cavity and the smaller by-product transport from the counter electrode that resulted from the highly viscous alginate sol electrolyte acting as a barrier for the mass transfer of oxygen molecules and electrochemical by-products [23,24].

3.3. Measurement of cell respiration activity

In general, most suspended cells must undergo the processes of sedimentation, adhesion, spreading and proliferation on a substrate for the maintenance of life [31]. The cells staying in various statuses, such as approach, adhesion and spreading, could lead to different activities. Most mammalian cells on a cell-adhesive, protein-coated matrix [36] or amino group-modified substrate [31] can complete the adhesion process within 6 h. In the study, we carried out a time-lapse measurement of the oxygen consumption of HeLa cells to realise the change in respiration activity during the cell-adhesion process. Fig. 5A shows that the reduction current of dissolved oxygen was monitored over time following the seeding of a 10 μl HeLa cell suspension (3×10^5 cells/ml) in the 3 mm diameter reservoir that was initially filled with 50 μl DMEM solution. The curve (a) in Fig. 5A represents the change in the reduction current of oxygen before and after the cell seeding performed at around 330 s. Before the cell seeding, the dissolved oxygen concentration in the DMEM solution was measured. Owing to the quasi-steady state diffusion behaviour of the ultramicroelectrode [37] and less electrochemical

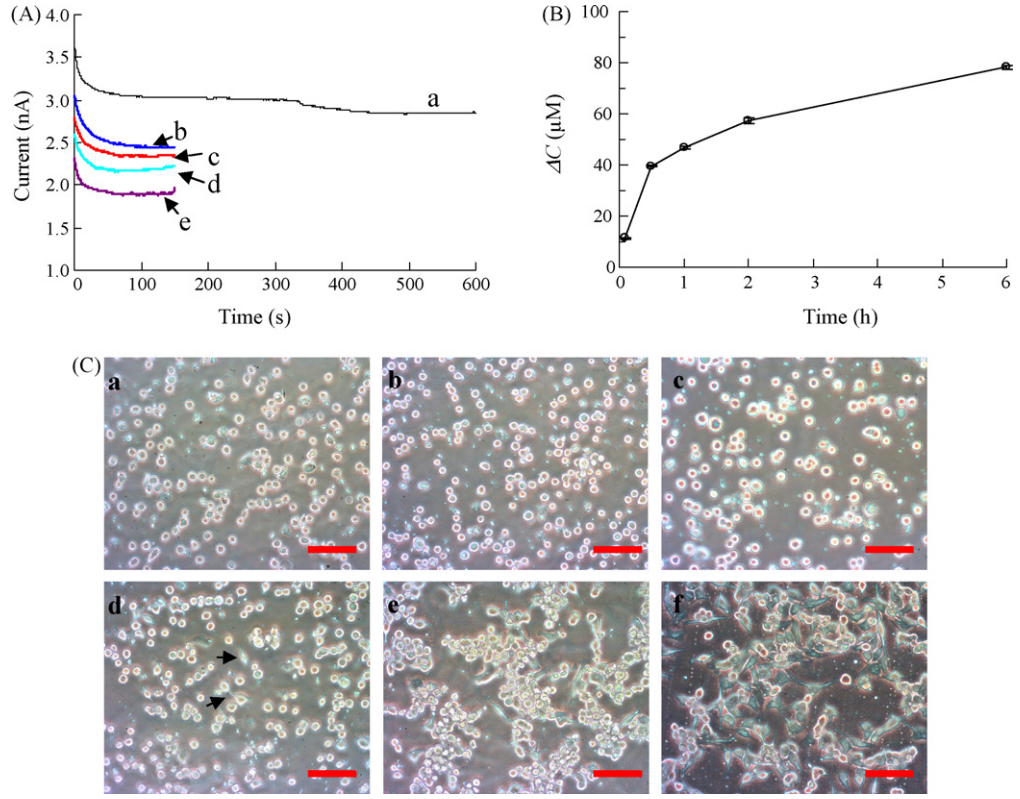

Fig. 5. The time-lapse reductive current of dissolved oxygen (A) and the oxygen consumption (ΔC) of HeLa cells (B) were recorded with time after seeding the cells on the Clark-type oxygen chip. Curve (a) was the current change before and after the HeLa cells were seeded onto the surface of the oxygen-permeable membrane at about 330 s. Curves (b)–(e) were obtained after seeding the cells for 30 min, 1 h, 2 h and 6 h, respectively. (C) The morphology of HeLa cells was observed with an inverted microscope after being seeded on the APTS-modified oxygen-permeable membrane for 5 min (a), 30 min (b), 1 h (c), 2 h (d), 6 h (e) and 18 h (f). Scale bar represents 100 μm.

crosstalk in the Clark-type oxygen chip, the measured current could quickly reach and maintain a stable value with little perturbation after applying the −0.7 V potential for 100 s. The cell suspension was placed at 330 s, and the reduction current gradually declined until 450 s, indicating that most cells can precipitate onto the OPM surface within 120 s. After the cells settled on the OPM surface, they began to undergo the adhesion process. The time-lapse change in reduction current in different cell-adhesion statuses was separately recorded for 150 s. Curve (b) to curve (e) of Fig. 5A correspond to 30 min, 1 h, 2 h and 6 h of incubation time after the cell seeding. The results show that the measured reduction current decreased with increasing incubation time, suggesting that the adhering cells increasingly consumed the dissolved oxygen. Biologically, a living cell needs to consume oxygen to maintain life. When the cells are more active, the rate of oxygen consumption becomes faster, leading to a lower dissolved oxygen concentration [10,15]. In the last 50 s period of each current measurement, curves (a)–(e) presented a relatively stable value that was adopted to statistically calculate the oxygen concentration of the media. The oxygen consumption (ΔC) of cells was used to estimate the cellular respiration activity and expressed as

$$\Delta C = C^* - C_{cell} \quad (1)$$

where C^* and C_{cell} are the dissolved oxygen concentration of the cell-free and cell-seeding DMEM solutions, respectively. C^* is 214 μM at 37 °C [17]. C_{cell} can be calculated from

$$C_{cell} = C^* \left(\frac{I_{cell}}{I^*} \right) \quad (2)$$

where I^* and I_{cell} are the reduction current of oxygen measured in the cell-free and cell-seeding DMEM solutions, respectively. Fig. 5B shows the change in the oxygen consumption of HeLa cells after seeding the cells for 5 min, 30 min, 1 h, 2 h and 6 h, respectively. The results show that the amount of oxygen consumed increased with time after seeding, implying that the cells in the cell-adhesion process gradually increased their respiration rate to generate more energy (ATP) by consuming more oxygen. Moreover, the increment of oxygen consumption per minute became smaller and smaller after 30 min of incubation. This increase in oxygen consumption is analogous to the cell-adhesion behaviours observed in Arima and Iwata's study, where the time course was observed with a total internal reflection fluorescent microscope [31]. For example, Arima and Iwata proved that most cells (over 90%) could adhere to the amino group-modified surface within 1 h of incubation and then slowly increase with time, and the average adhesion area for a cell clearly enlarged within 1 h and then slowly approached the maximum spreading at 3 h. Therefore, the oxygen consumption of cells is positively related to the cell-adhesion process. Nevertheless, the respiration rate of cells measured with the planar oxygen sensors of the Bionas® metabolic chip continuously declined within the first 2 h period and then increased with time after 2 h of incubation [15]. This unreasonable result is probably caused by the change in the electrochemical properties of the sensing area of the working electrode due to the coverage or contamination of cells and proteins. Therefore, our Clark-type oxygen chip can monitor in real time the change in the oxygen consumption of cells from the seeding to the adhesion process, and it possesses a good potential to distinguish the effects of different extracellular matrices on the cell-adhesion process.

Fig. 5C shows the time-lapse morphological images of HeLa cells cultured on the APTS-modified OPM substrate. Most cells could land on the surface within a 5 min period because the cell density observed from at 5 min (738 cells/mm^2) to at 30 min (848 cells/mm^2) only increased by 15%. Similarly, Arima proved that the cells can settle on the substrate within 5 min with the facilitation of gravity and medium convection [31]. To compare the increment of oxygen consumption with the number of cells landing in a varied interval, the increment of oxygen consumption in the 5–30 min interval was 2.44 times larger than that in the 0–5 min interval (Fig. 5B), but the density of landing cells only increased by 15%. The results imply that some cells adhering to the APTS-modified surface activate a signal transduction to increase oxygen consumption, although most cells presented a round-like shape and kept almost the same contact area as was observed at 5 min. After incubating for 1 h, the cells presented the larger area necessary to prepare for spreading onto the surface. After 2 h of incubation, a few cells (as indicated by arrows in Fig. 5C(d)) began to spread and the ratio of spreading cells increased with time. After 18 h of incubation, most cells presented elongated and irregular shapes, implying that the cells grew well on the amino group-modified OPM surface in a good adhesion status.

In order to evaluate the effect of chemicals on the cell activity in the good cell-adhesion status, HeLa cells with a 4.3×10^2 cells/mm^2 density were cultured on the APTS-modified OPM surface of the Clark-type oxygen chip for 18 h. Before the drug-sensitivity experiment, only 15 μl DMEM solution was left in the reservoir. The effect of chemicals, such as glucose and propofol, on the respiration activity of HeLa cells in a temperature-controlled incubator (37 °C) is shown in Fig. 6. The cellular respiration activity is defined by the change in the oxygen consumption of cells induced by a chemical stimulant normalised by the original oxygen consumption of cells in stimulant-free DMEM solution. A spike signal always occurred after dropping the chemicals into the reservoir, which is attributed to the effect of flow convection. Placing 10 μl Dulbecco's phosphate-buffered saline containing 100 mM glucose into the reservoir can instantly increase the glucose concentration from 25 mM to 55 mM. When the cells were exposed in the 55 mM glucose solution, the respiration activity increased with time and reached a plateau, with the 2.6% maximum increment after 8.5 min of exposure time. The result implies that HeLa cells can gradually increase their oxygen consumption in a solution containing a higher glucose concentration. Subsequently, 10 μl of propofol (10 mg/ml), an intravenous anaesthetic, was added to the reservoir at 20 min and 30 min in the activity curve of Fig. 6. The addition of propofol caused the respiration activity of the cells to decrease with time (to as low as 94.7%) due to the inhibition of ATP synthesis in the mitochondria [38]. Furthermore, the respiratory activity was drastically decreased at 36 min; this is attributed to the detachment of cells because in Mammoto et al.'s study, the administration of propofol inhibited the formation of the actin stress fibres and the focal adhesion of HeLa cells [39]. Moreover, the HeLa cells were observed to present a round-like shape after the experiment.

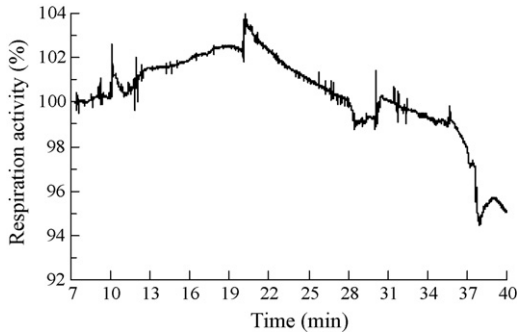

Fig. 6. The effect of chemicals on the respiratory activity of HeLa cells (4.3×10^2 cells/mm^2) was estimated in real time after cultivating the cells on the Clark-type oxygen chip for 18 h. 10 μl glucose (100 mM) was added at 10 min and 10 μl propofol (10 mg/ml) was separately added at 20 min and 30 min. The previous 7-min signal was omitted after applying the reductive potential.

The Clark-type oxygen chip can measure in real time the respiration activity of HeLa cells that were cultured *in situ* on the APTS-modified OPM to prevent the external medium from contaminating the amperometric electrodes. Moreover, the Clark-type oxygen chip is easily integrated with a PDMS micro-channel by using the same fabrication processes. This has the potential to be developed into a miniature flow-injection-analysis system to perform high throughput detection for tumour chemosensitivity tests or drug screening.

4. Conclusion

In this study, a Clark-type oxygen chip integrated with an OPM-separated reservoir was constructed to measure *in situ* the respiration activity of adhering HeLa cells. The use of the alginate sol electrolyte effectively diminishes the crosstalk between the electrochemical electrodes to obtain only 1.00% residual current but extends the response time by about 13.4 s. The electroplated thick-film Ag/AgCl reference electrode possessing the relatively large area can supply a more stable potential for the reduction of dissolved oxygen. The OPM surface silanised by the APTS molecules could present amino groups, which facilitate the adherence of HeLa cells to the surface of the PDMS OPM. The respiration activity of cells in the cell-adhesion process can be realised by directly measuring the oxygen consumption of cells with the Clark-type oxygen chip. It is useful to explore the relationship between the different cell lines and the varied extracellular matrix. Moreover, the effect of chemical stimulants on the respiration activity of cells can be specifically estimated, without any external interference resulting from additional electrochemical reactions of the stimulants, contamination of electrodes and change of the medium composition.

Acknowledgements

This work was supported by grants from the National Science Council (NSC94-2218-E-005-018 and NSC98-2213-B-005-031-MY3), from the Taichung Veterans General Hospital and National Chung Hsing University (TCVGH-NCHU 967609) and in part by the Ministry of Education, Taiwan, ROC under the ATU plan, Taiwan.

References

[1] T. Haruyama, Adv. Drug Deliv. Rev. 55 (2003) 393.
[2] R.A. Yotter, D.M. Wilson, IEEE Sens. J. 4 (2004) 412.
[3] P. Wang, G. Xu, L. Qin, Y. Xu, Y. Li, R. Li, Sens. Actuators B: Chem. 108 (2005) 576.
[4] F. Hafner, Biosens. Bioelectron. 15 (2000) 149.
[5] W.H. Baumann, M. Lehmann, A. Schwinde, R. Ehret, M. Brischwein, B. Wolf, Sens. Actuators B: Chem. 55 (1999) 77.
[6] B. Wolf, M. Brischwein, W.H. Baumann, R. Ehret, M. Kraus, Biosens. Bioelectron. 13 (1998) 501.
[7] M. Lehmann, W. Baumann, M. Brischwein, H.-J. Gahle, I. Freund, R. Ehret, S. Drechsler, H. Palzer, M. Kleintges, U. Sieben, B. Wolf, Biosens. Bioelectron. 16 (2001) 195.
[8] I.A. Ges, B.L. Ivanov, D.K. Schaffer, E.A. Lima, A.A. Werdich, F.J. Baudenbacher, Biosens. Bioelectron. 21 (2005) 248.
[9] I.A. Ges, B.L. Ivanov, A.A. Werdich, F.J. Baudenbacher, Biosens. Bioelectron. 22 (2007) 1303.
[10] T. Henning, M. Brischwein, W. Baumann, R. Ehret, I. Freund, R. Kammerer, M. Lehmann, A. Schwinde, B. Wolf, Anti-Cancer Drugs 12 (2001) 21.
[11] M. Brischwein, E.R. Motrescu, E. Cabala, A.M. Otto, H. Grothe, B. Wolf, Lab Chip 3 (2003) 234.
[12] J. Wiest, M. Schmidhuber, J. Ressler, A. Scholz, M. Brischwein, B. Wolf, IFMBE Proc. 10 (2005) 132.
[13] A.M. Otto, M. Brischwein, A. Niendorf, T. Henning, E. Motrescu, B. Wolf, Cancer Detect. Prev. 27 (2003) 291.
[14] E.R. Motrescu, A.M. Otto, M. Brischwein, S. Zahler, B. Wolf, J. Cancer Res. Clin. Oncol. 131 (2005) 683.
[15] L. Ceriotti, A. Kob, S. Drechsler, J. Ponti, E. Thedinga, P. Colpo, R. Ehret, F. Rossi, Anal. Biochem. 371 (2007) 92.
[16] R.S. Balaban, Am. J. Phyiol. Cell Physiol. 258 (1990) C377.
[17] D.V. Heimbrug, K. Hemmrich, S. Zachariah, H. Staiger, N. Pallua, Respir. Physiol. Neurobiol. 146 (2005) 107.
[18] T. Kitahara, N. Koyama, J. Matsuda, Y. Hrakata, S. Kamihira, S. Kohno, M. Nakashima, H. Sasaki, Biol. Pharm. Bull. 26 (2003) 1229.
[19] E. Thedinga, A. Kob, H. Holst, A. Keuer, S. Drechsler, R. Niendorf, W. Baumann, I. Freund, M. Lehmann, R. Ehret, Toxicol. Appl. Pharmacol. 220 (2007) 33.
[20] M. Koudelka, Sens. Actuators 9 (1986) 249.
[21] H. Suzuki, N. Kojima, A. Sugama, F. Takei, K. Ikegami, Sens. Actuators B: Chem. 1 (1990) 528.
[22] H. Suzuki, A. Sugama, N. Kojima, Sens. Actuators B: Chem. 2 (1990) 297.
[23] H. Suzuki, A. Sugama, N. Kojima, Sens. Actuators B: Chem. 10 (1993) 91.
[24] H. Suzuki, H. Ozawa, S. Sasaki, I. Karube, Sens. Actuators B: Chem. 54 (1998) 140.
[25] H. Suzuki, H. Shiroishi, S. Sasaki, I. Karube, Anal. Chem. 71 (1999) 5069.
[26] H. Suzuki, T. Hirakawa, S. Sasaki, I. Karube, Anal. Chim. Acta 405 (2000) 57.
[27] H. Suzuki, H. Arakawa, I. Karube, Biosens. Bioelectron. 16 (2001) 725.
[28] Z. Yang, S. Sasaki, I. Karube, H. Suzuki, Anal. Chim. Acta 357 (1997) 41.
[29] C.C. Wu, T. Yasukawa, H. Shiku, T. Matsue, Sens. Actuators B: Chem. 110 (2005) 342.
[30] Y. Matsubara, Y. Murakamil, M. Kobayashi, Y. Morita, E. Tamiya, Biosens. Bioelectron. 19 (2004) 741.
[31] Y. Arima, H. Iwata, J. Mater. Chem. 17 (2007) 4079.
[32] B.J. Polk, A. Stelzenmuller, G. Mijares, W. MacCrehan, M. Gaitan, Sens. Actuators B: Chem. 114 (2006) 239.
[33] H. Shiku, T. Saito, C.-C. Wu, T. Yasukawa, M. Yokoo, H. Abe, T. Matsue, H. Yamada, Chem. Lett. 35 (2006) 234.
[34] C.R. Wilke, P.C. Chang, AIChE J. 1 (1955) 264.
[35] A.C. Hulst, H.J.H. Hens, R.M. Buitelaar, J. Tramper, Biotechnol. Technol. 3 (1989) 199.
[36] F. Grinnell, T.V. Phan, J. Cell Physiol. 116 (1983) 289.
[37] A.J. Bard, L.R. Faulkner, in: A.J. Bard (Ed.), Electrochemical Methods Fundamentals and Applications, 2nd ed., John Wiley & Sons, Inc., New York, 2000, p. 170.
[38] D. Branca, E. Vincenti, G. Scutari, Comp. Biochem. Physiol. C 110 (1995) 41.
[39] T. Mammoto, M. Mukaib, A. Mammotoc, Y. Yamanakab, Y. Hayashid, T. Mashimod, Y. Kishia, H. Nakamura, Cancer Lett. 184 (2002) 165.